JOURNAL OF GEOPHYSICAL RESEARCH, VOL. 100, NO. D11, PAGES 23,125–23,131, NOVEMBER 20, 1995

Ozone fluxes over a patchy cultivated surface

L. Mahrt,[1] D. H. Lenschow, Jielun Sun,[2] and J. C. Weil[3]
National Center for Atmospheric Research, Boulder, Colorado

J. I. MacPherson
Flight Research Laboratory, National Research Council, Ottawa, Ontario, Canada

R. L. Desjardins
Land Resources Research Centre, Agriculture Canada, Ottawa

Abstract. This study examines the spatial variability of ozone fluxes over flat heterogeneous terrain consisting of a patchwork of irrigated and nonirrigated surfaces. Fluxes of ozone and other quantities are computed from eight sequential flight legs of the Canadian Twin Otter research aircraft over the same track at 33 m above the surface for each of 2 days. The fluxes are composited over the eight runs to reduce the random flux error. The fluxes of heat, moisture, and carbon dioxide are closely related to spatial variations of surface vegetation. However, the ozone flux is affected by additional factors including reaction with NO released from point sources. This effect is illustrated here with two examples of irrigation pumping stations driven by diesel engines. We conclude that the ozone deposition to the surface cannot be estimated from the measured ozone flux without correction for the NO sources.

1. Introduction

The daytime boundary layer is typically characterized by downward turbulent flux of ozone. This downward ozone flux is partly associated with entrainment of ozone from the overlying layer [*Neu et al.*, 1994] and ultimately leads to deposition of ozone at the Earth's surface. Surface deposition of ozone onto vegetated and bare surfaces depends on factors different from those affecting surface fluxes of heat, moisture, and carbon dioxide [*Massman et al.*, 1994]. A large fraction of the ozone deposition is directly onto soil and leaf surfaces and is not part of the stomatal exchange [*Leuning et al.*, 1979; *Wesely*, 1983].

Ozone deposition also depends on the soil water content and atmospheric humidity. Since ozone is not very soluble in water, deposition of ozone to wet soils is less than for dry soils [*Chamberlain*, 1986] and becomes quite small over saturated soils [*Wesely et al.*, 1981]. *McLaughlin and Taylor* [1981] found that ozone deposition to plants can increase by a factor of 2 or 3 when relative humidity increases from 35% to 75%. As a result of these factors, the spatial variation of ozone fluxes may show a more complex relationship to spatial variations of vegetation cover and soil conditions than is shown by heat and moisture fluxes [e.g., *Massman et al.*, 1994; *Sun and Mahrt*, 1994]. For example, *Mahrt et al.* [1994] find that for the data set analyzed in this study, most of the variance of the heat and moisture flux is due to spatial variations of surface conditions, while most of the variance of the ozone flux is due to transient behavior.

There are situations, however, where the ozone flux is closely related to the vegetative cover and highly correlated with fluxes of heat, moisture, and carbon dioxide. For example, *MacPherson* [1992] found an approximate relation between ozone flux and the greenness index when comparing aircraft data collected at homogeneous sites over a 1-month observational period. Similarly, *Lenschow et al.* [1981] found a good qualitative relationship between ozone fluxes and vegetation over a region of mixed rangeland and irrigated cropland. In their case the grass was senescent and there were no apparent significant sources of NO.

As an additional complication, the flux measured above the surface may be considerably different from the surface flux. These differences may result from a large entrainment rate, horizontal advection, rapid time changes, or, in the case of chemically reactive species, production or loss of the species between the surface and the measurement height. Ozone can react with NO on timescales that are short enough to significantly modify the vertical divergence of the ozone flux.

Lenschow [1995] estimates the turbulent diffusion timescale to be of the order of a couple of minutes in the upper part of a convective surface layer (lowest 30 m), and a few tens of minutes up to an hour in the overlying mixed layer (1 or 2 km depth). This means that the reaction of ozone with NO, which has a time constant of roughly a couple of minutes, can significantly alter the ozone flux measured, even within the surface layer [*Lenschow*, 1982; *Fitzjarrald and Lenschow*, 1983; *Lenschow and Delany*, 1987; *Kramm et al.*, 1991].

A major source of NO is combustion. Therefore its emission is inherently inhomogeneous and often episodic. When first released, it reacts quickly with ozone and, in large concentrations, can effectively remove the ozone. This is a transient effect. Eventually, as the air is diluted and the NO reaches

[1]Now at College of Oceanic and Atmospheric Sciences, Oregon State University, Corvallis.
[2]Now at Program in Atmospheric and Oceanic Sciences, University of Colorado, Boulder.
[3]Now at Cooperative Institute for Research in Environmental Sciences, University of Colorado, Boulder.

Paper number 95JD02599.
0148-0227/95/95JD-02599$05.00

photochemical equilibrium with NO_2, ozone, and various reactive hydrocarbons (and partially oxidized hydrocarbons), the ozone concentration may reach even higher values than were present before the introduction of NO. This is due to ozone production on longer timescales by other chemical processes (e.g., reactions with hydrocarbons) that are enhanced by NO [*Seinfeld*, 1986].

This paper investigates the relationship of measured ozone fluxes to surface variability in contrast with the relationship of heat and moisture fluxes to the same surface variability. A major goal of this study is to evaluate the ability of the aircraft to estimate spatially averaged surface ozone fluxes in the presence of chemical reactions between the aircraft level and the surface. Surface conditions will be posed in terms of the normalized difference of vegetation index (NDVI) as described by *Tucker* [1979]. The next section describes how the fluxes and NDVI are computed from aircraft data.

2. Data Description and Flux Computations

We analyze data from flights of the Twin Otter aircraft operated by the Canadian Flight Research Laboratory of the National Research Council. The instrumentation is described by *MacPherson* [1992] and *MacPherson et al.* [1993]. The aircraft measurements were obtained at 33 m above flat ground, which is near the top of the surface layer. The underlying surface consists of a patchwork of relatively cool, moist irrigated fields and hot, dry nonirrigated fields. Ozone measurements were carried out using the Deutsche Forschungsanstalt für Luft- und Raumfahrt (DLR) fast response ozone analyzer [*Schmidt et al.*, 1991]. This analyzer is based on a surface chemiluminescent reaction of ozone with a selected organic dye absorbed on an aluminum disk coated with a dry silica gel. These measurements were compared with the fast response ozone detector described by *Pearson and Stedman* [1980]. Both instruments agreed well with each other in terms of overall spatial structure. We arbitrarily report results only from the DLR sensor. The instrument root-mean-square (rms) noise level was estimated to be less than 0.1 ppb and is thought not to be a factor in the following analysis.

The data were collected during the California Ozone Deposition Experiment (CODE) in the San Joaquin Valley of California about 100 km south of Fresno. The same flight track was repeated eight times during each of 2 clear days; July 23, 1991 (flight 13), and July 30, 1991 (flight 19). Winds at the 33-m flight level were from the northwest at about 4 m s^{-1} during flight 13 and light with variable wind direction during flight 19. The eight legs for flight 13 were flown between approximately 1300 and 1500 local solar time, while the eight flight legs for flight 19 were flown between approximately 1045 and 1245 local solar time. Flight 13 was less influenced by diurnal variation because of the stronger wind and later time of day. For flight 19, *Mahrt et al.* [1994] find that about 10% of the flux variance is due to diurnal variation.

The irrigated and nonirrigated areas under the flight track are delineated as depicted in Figure 1 using the NDVI as a measure of the variation of surface vegetation [*Tucker*, 1979]. It is computed here from aircraft-measured reflectance at two wavelengths, one centered at 0.73 μm and the other at 0.66 μm. The surface heterogeneity in CODE is well defined by the NDVI (Figure 1) which is highly negatively correlated with the surface radiation temperature. The surface radiation temperature is about 20°C cooler over the irrigated croplands compared with the nonirrigated areas, similar to the variation shown by *Doran et al.* [1992]. The air temperature at 33 m for flight 19 varies by 2°–3°C between irrigated and nonirrigated areas and by about 1.5°C for flight 13.

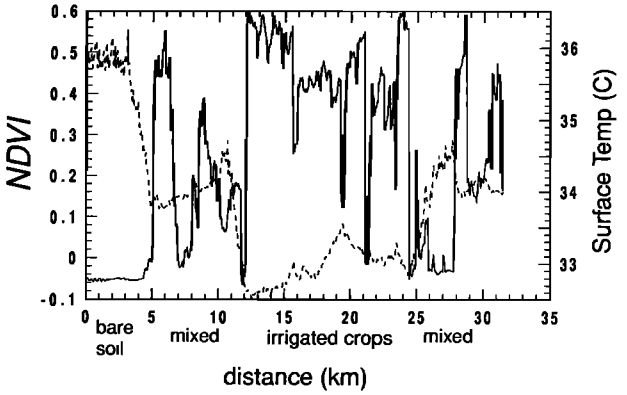

Figure 1. Normalized difference of vegetation index (NDVI) (solid line) and air temperature at 33 m (dashed line) filtered with a moving average window with width of 375 m and composited over all of the flight legs for flight 19 (defined as $\{\phi(x, t)\}$ in section 2). Northeast (southwest) is directed to the right (left).

To estimate fluxes from the aircraft data, we first define a moving average $[\phi(x, t)]$, where x is the distance along the aircraft leg and $\phi(x, t)$ represents one of the velocity components, temperature, moisture or chemical species. The total flow is then decomposed as

$$\phi(x, t) = [\phi(x, t)] + \phi'(x, t)$$

where $\phi'(x, t)$ is the turbulent part of the signal computed as deviations from $[\phi(x, t)]$. We define the operator $[\phi(x, t)]$ to be an equally weighted moving average with window width of either 375 m (100 points at the sample rate of 16 s^{-1}), 1 km, or 5 km and then compute the turbulent flux $[w'(x, t)\phi'(x, t)]$. This window is sequentially translated one point at a time (approximately 3.5 m). A window width of 375 m omits a significant fraction of the turbulent flux but provides good spatial resolution over the heterogeneous surface. Window widths of 1 km and 5 km capture most of the turbulent flux [*Sun and Mahrt*, 1994] but have poorer spatial resolution.

To estimate the contributions of the surface heterogeneity, we reduce the influence of transient mesoscale motions by compositing $[\phi(x, t)]$ and $[w'\phi']$ over all eight aircraft legs to obtain $\{[\phi(x, t)]\}$ and $\{[w'\phi']\}$, where the operator $\{\ \}$ indicates an average over all of the flight legs at a given location x. Therefore the average of the spatial distribution over all of the runs, $\{[\phi(x, t)]\}$, is an estimate of the stationary part of the spatial variation. However, it still contains significant transient fluctuations which are not completely removed by the compositing. The estimate of the stationary part of the turbulent fluxes is computed by compositing $[w'\phi']$ over the eight flight legs to obtain $\{[w'\phi']\}$ for each location. Since $[w'\phi']$ is not smoothed before compositing, it also includes significant small-scale variations that were only partially removed by the compositing. Flux errors due to limited sample size for the composited spatial distribution are discussed by *Sun and Mahrt* [1994]. The flux sampling errors for an individual run at a given point location are large, and we currently have no technique to quantitatively estimate them.

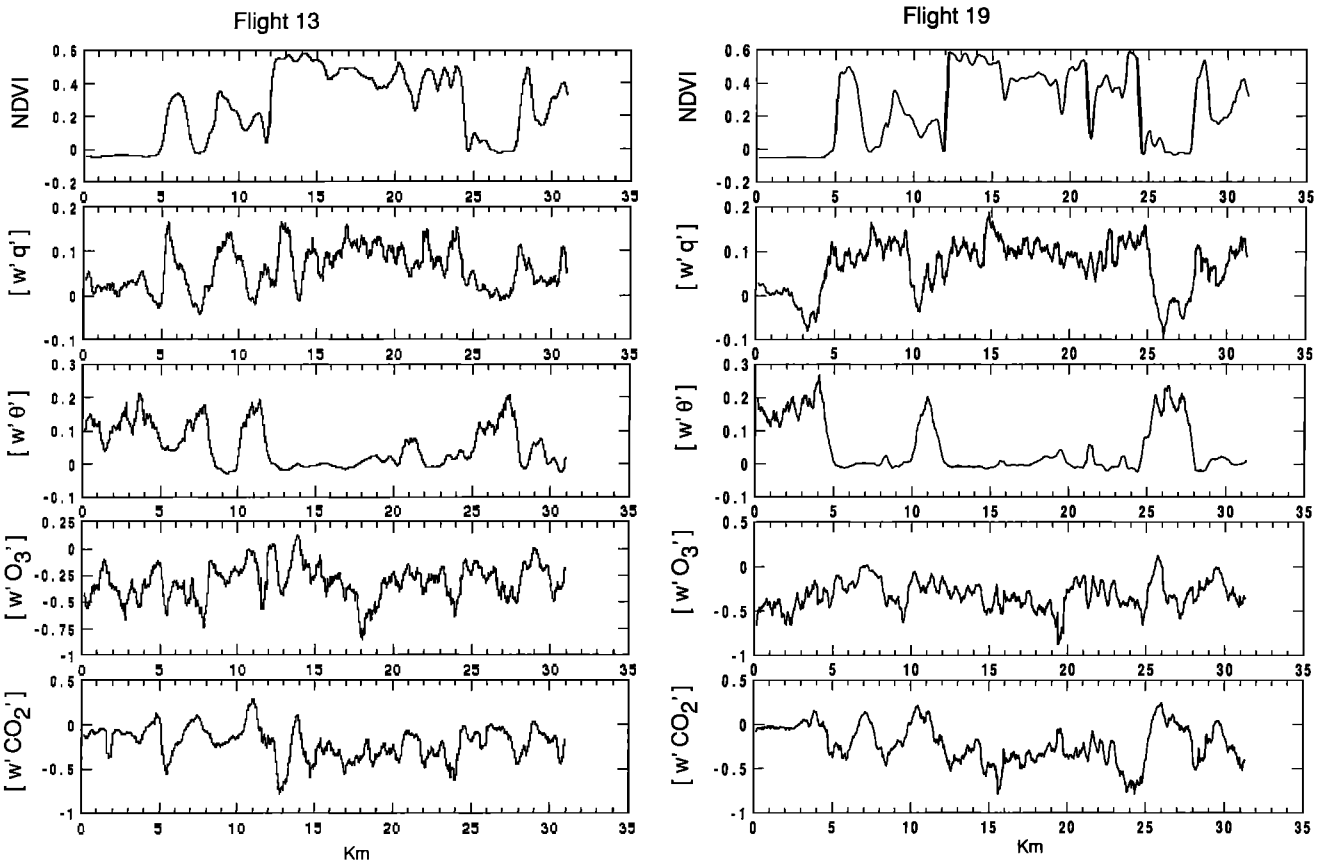

Figure 2. Composited spatial variation of the NDVI, specific humidity flux $[w'q']$ (m s^{-1} g kg^{-1}), temperature flux $[w'\theta']$ (m s^{-1} °K), ozone flux $[w'O_3']$ (m s^{-1} ppb), and carbon dioxide flux $[w'CO_2']$ (m s^{-1} mg kg^{-1}) computed from deviations from a moving average with a 375-m window width for flights 13 and 19.

3. Fluxes and Remotely Sensed Variables

In this section we examine the spatial variation of the composited fluxes (Figure 2). We also consider the spatial correlation between the composited fluxes and the remotely sensed NDVI and surface radiation temperature. If these fluxes are controlled mainly by transpiring vegetation, we would expect to see high positive correlation between the NDVI and moisture flux, and high negative correlation between the NDVI and fluxes of heat, CO_2, and ozone. For flight 13 the magnitudes of the heat, moisture, and CO_2 fluxes are significantly correlated with the remotely sensed surface variables (Table 1). In contrast, the ozone flux is poorly correlated with surface variables, particularly at the 1-km scale. The ozone flux is more highly correlated with the NDVI at the 5-km scale (Table 1). The ozone flux is somewhat more highly correlated with the surface variables for flight 19 (not shown) but still much less correlated compared with the heat, moisture, and carbon dioxide fluxes.

The smaller correlation of the ozone flux with the NDVI may be related to local interactions with NO_x and/or direct deposition of ozone onto soil and leaf surfaces, independent of stomatal activity. In support of the latter possibility, *Leuning et al.* [1979] have shown that direct deposition to leaf surfaces and the soil can account for as much as half of the total ozone flux over vegetated surfaces. In the case study of *Wesely* [1983, Table 5], the surface resistance to ozone uptake is only slightly greater over bare soil than over cropland.

Since surface temperature and NDVI are highly (negatively) correlated (Table 1), the correlations of the fluxes with the remotely sensed surface temperature are numerically close to the corresponding correlations with the NDVI. For the 5-km window, the ozone flux is modestly (negatively) correlated with the fluxes of heat and moisture and more significantly correlated with the carbon dioxide flux, possibly indicating the contribution of stomatal control. However, most of the variance of the ozone flux seems related to other factors. In the next section we show how some of the variability of the ozone flux is related to surface sources of NO.

4. Ozone Chemical Sinks

Since ozone reacts very quickly with NO, any region containing a source of NO can perturb the ozone flux profile. This may cause significant differences between ozone flux measurements at the surface and at some height above the surface. Previous studies [e.g., *Fitzjarrald and Lenschow*, 1983; *Lenschow and Delany*, 1987; *Kramm et al.*, 1991] have shown how surface fluxes of O_3, NO, or NO_2 can perturb the photochemical equilibrium of these species, resulting in divergence of their flux profiles and changes in their mean concentrations. Furthermore, *Lenschow et al.* [1981] showed an example of anomalous negative spikes in ozone concentration at 150 m above the surface, which coincided with positive w fluctuations along a flight leg in close proximity to a highway.

In the present study, large downward ozone fluxes occurred over regions of less than 1-km width at the aircraft flight level on both flights 13 and 19 (Figure 3). For further study we select

Table 1. Correlation Coefficients

	q	T_A	NDVI	T_S	$[w'\theta']$	$[w'q']$	$[w'CO_2']$
			1-km Window				
T_A	−0.929						
NDVI	0.752	−0.848					
T_S	−0.756	0.812	−0.889				
$[w'\theta']$	−0.637	0.753	−0.839	0.922			
$[w'q']$	0.729	−0.755	0.787	−0.891	−0.901		
$[w'CO_2']$	−0.675	0.776	−0.850	0.778	0.764	−0.794	
$[w'O_3']$	0.083	−0.116	−0.125	−0.103	−0.119	−0.054	0.266
			5-km Window				
T_A	−0.935						
NDVI	0.917	−0.941					
T_S	−0.899	0.839	−0.894				
$[w'\theta']$	−0.749	0.754	−0.837	0.928			
$[w'q']$	0.753	−0.814	0.805	−0.875	−0.949		
$[w'CO_2']$	−0.645	0.827	−0.780	0.618	0.698	−0.797	
$[w'O_3']$	−0.437	0.613	−0.659	0.381	0.522	−0.573	0.823

Here, q is specific humidity, T_A is air temperature, NDVI is normalized difference of vegetation index, T_S is surface temperature, $[w'\theta']$ is heat flux, $[w'q']$ is moisture flux, $[w'CO_2']$ is carbon dioxide flux, and $[w'O_3']$ is ozone flux.

the location of largest downward ozone flux for each of the two flights. The aircraft intersects the enhanced downward ozone flux on only two of the runs where the downward flux is considerably larger than in the composited profile.

For the run with the most definable event of large downward ozone flux during flight 13, we estimate the flux to be 1.2 ppb m s^{-1} over a 500-m segment. If this flux represents a localized plume of large downward ozone flux resulting from a point source of NO, then the aircraft data would underestimate the maximum downward flux and the width of the plume if the

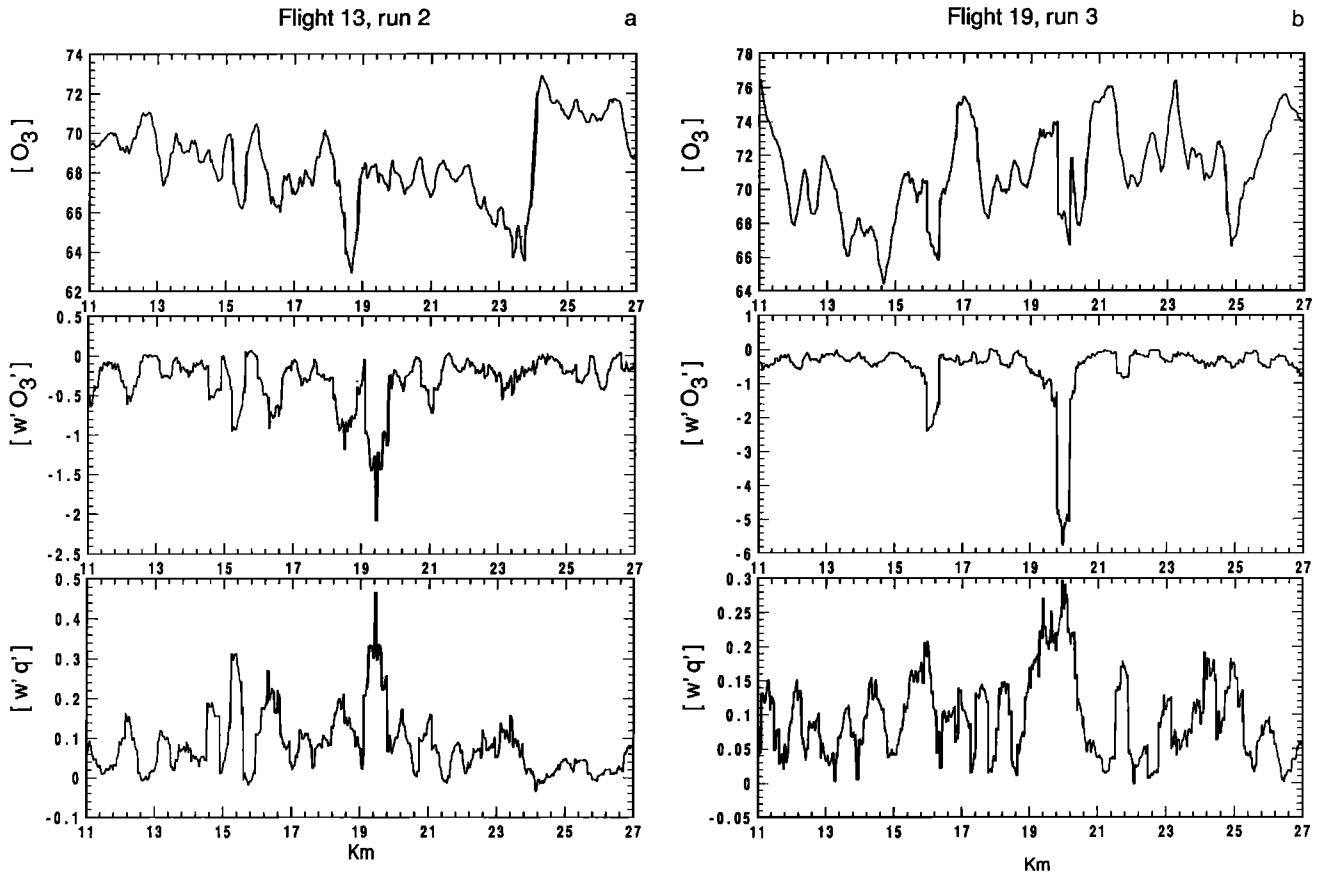

Figure 3. Spatial variation of ozone concentration for the flight run with largest downward ozone flux for (a) flight 13 and (b) flight 19. The ozone concentration is computed from a moving average translated one point at a time (approximately 3.5 m) with a window width of 375 m for ozone (parts per billion), specific humidity (grams per kilogram), and the NDVI.

aircraft did not fly through the center of the plume. On the other hand, the aircraft could overestimate the width of the plume if it flew obliquely through the plume. Smoothing associated with the 375-m window artificially reduces the amplitude of the downward ozone flux and increases the computed width of the plume. Decreasing the window width increases the amplitude of the flux peak but leads to noisier spatial distribution of the flux. The instantaneous flux shows several subplumes of strong flux occurring over a horizontal distance of 500 m. Fortunately, the total transport is not very sensitive to the choice of window width, so that the estimation of the ground source is relatively robust. With the aforementioned difficulties in mind and assuming a flux value of 1.2 ppb m s^{-1} is representative of a 500-m square, the computed flux corresponds to a total integrated areal ozone loss of about 4.8×10^{-4} kg s^{-1}, or 1.8 kg h^{-1}.

The spatial position of the large downward ozone flux for flight 13 does not coincide with the position of the large ozone deficit. This is probably because the mean ozone concentration results mainly from the time integral of the flux divergence rather than from the instantaneous flux.

The enhanced downward flux of ozone for flight 19 was also observed mainly on one run (Figure 3b). Even though the spatial variation of the fluxes for an individual run is quite noisy, the region of maximum downward ozone flux is quite clear. The downward ozone flux reaches 5 ppb m s^{-1} over a 400-m-wide area. This integrated flux corresponds to a surface sink of about 1.3×10^{-3} kg s^{-1}. The 400-m-wide region of large downward flux of ozone coincides with a region of ozone deficit of about −5 ppbv. From instantaneous 16 s^{-1} data, this ozone deficit is found to result mostly from a concentrated plume of −40 ppbv ozone deficit over a 50-m width. The 400-m thickness of the plume width estimated above is influenced by the 375-m window used to compute the flux.

The small region of large downward ozone flux can contribute significantly to the area-averaged ozone flux. For example, consider the run for flight 19 where large downward ozone flux of 5 ppb m s^{-1} occurs over a 400-m segment. This flux event increases the spatially averaged flux over the 16-km irrigated region by about 32% compared with the value obtained without the flux event. The influence of this plume is considerably reduced in a time-space average using all of the flight runs. However, this time average appears to capture additional lesser events of large ozone flux probably related to vehicles or other pumps in the area. Similar conclusions are reached for flight 13. These observations suggest that the spatially averaged ozone flux measurement significantly overestimates the ozone deposition to the natural vegetated surface because of the ozone loss resulting from NO releases.

We assume that the source of NO needed to consume this amount of ozone is released as a point source. The immediate impact of a release of concentrated NO into a volume of air in which NO, NO_2, and O_3 are in photochemical equilibrium is to react with ozone and form NO_2. Within a few minutes the three species reach a new equilibrium, in which the ozone is reduced at the expense of increased NO_2 and NO. The air with decreased ozone mixes upward, resulting in the observed downward ozone flux. The timescale for this mixing is of the order of a few tens to a few hundred seconds, depending on the altitude [*Lenschow*, 1995].

The photochemical sequestering of O_3 in sunlight by NO emission can be estimated from the rate equations

$$O_3 + NO \rightarrow NO_2 + O_2 \quad (1)$$

$$O_2 + O \rightarrow O_3 \quad (2)$$

$$NO_2 + h\nu \rightarrow NO + O \quad (3)$$

where $h\nu$ is a photon of sufficient energy to photolyze NO_2. Reaction (2) is sufficiently fast that (2) and (3) can be combined, so that neglecting other slower reactions involving these species, the concentration budget of O_3 can be expressed as

$$d[O_3]/dt = k_3[NO_2] - k_1[O_3][NO] \quad (4)$$

where k_1 and k_3 are the reaction coefficients of (1) and (3), respectively. Similar equations hold for NO and NO_2. If we neglect other competing reactions, rapid light intensity changes, and concentration fluctuations, then the right-hand side of (4) is approximately zero, so that

$$[O_3][NO]/[NO_2] = k_1/k_2. \quad (5)$$

This is the so-called photostationary state relation [*Seinfeld*, 1986].

We now consider the injection of NO from a surface point source into the boundary layer. As released NO mixes into the boundary layer, it reduces the ambient O_3 concentration through reactions (1)–(3). We assume that the mixing is slow enough that chemical equilibrium is reached as the mixing takes place. Since the reaction time constant is of the order of 100 s, this is a reasonable assumption except within a few meters of the source [*Lenschow*, 1995]. We describe this process by the following relations:

$$([O_3] + \delta[O_3])([NO] + \delta[NO])/([NO_2] + \delta[NO_2]) = [O_3][NO]/[NO_2] = k_3/k_1 \quad (6)$$

$$\delta[NO] + \delta[NO_2] = \alpha\delta[NO] \quad (7)$$

$$\delta[O_3] + \delta[NO_2] = 0 \quad (8)$$

The quantities $\delta[\ ]$ are the perturbations in $[O_3]$, [NO], and $[NO_2]$ introduced by the point source release of NO denoted by $\alpha\delta$[NO]. Equation (7) is the conservation equation for odd nitrogen, and (8) is the result of the stoichiometric reaction of O_3 with NO [*Seinfeld*, 1986].

Solving these equations for $\alpha\delta$[NO] as a function of $\delta[O_3]$ and the background concentrations, we obtain

$$\alpha\delta[NO] = -\delta[O_3][A + 1] \quad (9)$$

where

$$A = \{(k_3/k_1) + [NO]\}/\{[O_3] + \delta[O_3]\}$$

To estimate the magnitude of A in (9), we note that the observed mean concentration O_3 is about 70 ppbv (Figure 3), a typical deficit $\delta[O_3]$ on the scale of the 375-m window is about −5 ppbv, and a typical clear daytime value of k_1/k_2 is about 10 ppbv [*Seinfeld*, 1986]. Then the value of $\alpha\delta$[NO] is 5.84 ppbv for [NO] = 1 ppbv and 6.54 ppbv for [NO] = 10 ppbv. For concentrations of [NO] that are likely present here, A is small compared with 1 and $\alpha\delta[NO] \cong -\delta[O_3]$. The validity of this approximation depends on scale. For example, the approximation given above breaks down locally when we consider the largest ozone deficit on the scale of a few tens of meters, which was closer to −50 ppbv.

The discussion above suggests that a likely source of the observed O_3 deficits is a point release of NO. The maximum

downward ozone fluxes for both flights were located over sites with diesel engines driving pumping stations. The diesel pumps were located with the downward looking video camera and the use of detailed maps. The network of canals and patchwork of fields allowed unambiguous ground identification of the pumping systems, although the connection between the aircraft observed plume and the pumping stations cannot be categorically proven.

In examining the regulations for allowable emissions from nonhighway heavy-duty diesel engines for California, the values are in the range of 6.9–10.7 g of equivalent NO_2 per brake hp hour (D. Stedman, personal communication, 1994), where 1 hp = 746 W. The engine emits predominantly NO, but the units of measurement are equivalent grams of NO_2. If we assume an engine running at the allowable maximum standard of 10.7 g (brake hp h)$^{-1}$, the estimated ozone sink of 1.8 kg h^{-1} would result from an engine running at 160 hp.

We therefore investigated the possibility of a large stationary diesel engine operating in this area. We then found that for flight 13, a 70- to 100-hp Allison diesel engine, used to drive a tile drain pump, was located underneath the airplane flight track at the approximate location of the strong downward ozone flux. The pump automatically turns off and on depending on water levels and was apparently on for at least one of the eight flights.

For flight 19, the largest downward ozone flux (Figure 2) is about 1 km farther east near a canal and corresponds to an ozone sink 2–3 times larger than that during flight 13. At the location of this ozone sink for flight 19, two portable irrigation pumps were located, which were driven by 150-hp diesel engines. The large upward moisture flux over this area (Figure 3b) may be due to current irrigation of the underlying fields. On the basis of these calculations, we conclude that the most likely source of such a concentrated ozone loss was large, stationary diesel engines.

5. Plume Dispersion

In this section we make a rough estimate of the distance from the NO source to the aircraft-measured ozone flux. The flux measured by the aircraft is from a "quasi-instantaneous" plume rather than an Eulerian-averaged plume which would be obtained by a set of fixed-point measurements. The instantaneous plume is a problem in relative dispersion represented by the rms spread σ_r about the moving plume centroid, whereas the Eulerian-average plume is a problem in absolute dispersion represented by the rms spread σ_a relative to a fixed (absolute) coordinate system. Both rms values σ_r and σ_a are evaluated at a fixed point in the downstream direction and related by the expression $\sigma_a^2 = \sigma_m^2 + \sigma_r^2$, where σ_m is the rms meander of the instantaneous plume at a fixed point in the downstream direction.

Dispersion from a surface source is complicated by the height dependence of the turbulence length (l_e) and time (τ) scales, and the velocity variances. For a surface source, σ_a can be predicted using a z-dependent diffusivity $K(z) = l_e\ \tau$ provided that $\sigma_a \geq l_e$ [*van Ulden*, 1978; *Venkatram*, 1988].

In a similar way, K theory could be used for predicting σ_r, but observations of σ_r as a function of x would be required to determine a proportionality constant. Instead, we choose a simpler approach and estimate σ_r from a prediction of σ_a, using *Taylor*'s [1921] statistical plume model and the ratio σ_r/σ_a obtained from *Gifford*'s [1959] meandering plume model. Gifford's model describes the rms σ_c and mean C concentration fields due to the wandering of an instantaneous plume by the large eddies in a turbulent flow. Along the plume centerline, the model predicts that the fluctuation intensity σ_c/C is given by

$$\sigma_c^2/C^2 = \sigma_m^4/[\sigma_r^2(\sigma_r^2 + 2\sigma_m^2)] = 1/[f^2(f^2 + 1)] \qquad (10)$$

where $f = \sigma_r/\sigma_m$. Since $\sigma_m = \sigma_a/(1 + f^2)^{1/2}$, one can write $\sigma_r = \alpha^*\sigma_a$, where $\alpha^* = f/(1 + f^2)^{1/2}$. According to *Taylor*'s [1921] short-range result, absolute dispersion in the cross-wind (y) direction becomes $\sigma_{ay} = \sigma_v x/U$, where σ_v is the rms lateral turbulence velocity and U is the mean wind speed. The relative dispersion σ_{ry} in the cross-wind direction is then

$$\sigma_{ry} = \alpha^*\sigma_v x/U \qquad (11)$$

The $\alpha^*(f)$ required in (11) can be estimated using *Fackrell and Robin*'s [1982] wind tunnel measurements of σ_c/C due to a surface tracer release in a neutral boundary layer. Their data showed that along the plume centerline ($y = z = 0$), σ_c/C is approximately 0.6 and is independent of x over the range $1 \leq x/H \leq 6$, where H is the boundary layer height. The invariance of σ_c/C with x can be explained by a constant ratio $f = \sigma_r/\sigma_m$ in (10). With $\sigma_c/C = 0.6$, f is approximately unity and α^* is approximately 0.7.

For flight 19, where the wind is approximately perpendicular to the flight track, the observed instantaneous plume width Δy inferred from the instantaneous spatial distribution of the aircraft measured ozone flux is 50 m. Assuming a Gaussian spatial distribution and defining the width Δy to be the region where the concentration exceeds 10% of the peak value, we obtain the observed relative dispersion from the approximation $\sigma_{ry} = \Delta y/4.3$ which yields $\sigma_{ry} = 11.6$ m. Using measured values of $\sigma_v = 0.51$ m s^{-1}, $U = 2$ m s^{-1}, and $\alpha^* = 0.7$, (11) yields $x = 65$ m.

Intermittency of the pump operation, slight variations in the flight track or the effect of variable wind direction on the plume might explain the observation that the plume at aircraft level was either less defined or nonexistent on seven of the eight runs for flight 19. Generally, the light winds were normal to the flight track, in which case the aircraft may have flown over the plume on most of the runs. The best defined plume was observed when the wind vector had shifted around to about 30° from the flight track, in which case the aircraft intersected the plume downwind from the NO source.

The small sample size of flux data within the plume is a serious problem for the present study, and the choices of some of the numerical values given above are uncertain. Future aircraft measurements need to intentionally interrogate a plume having a known NO source with many repeated flight legs parallel with the wind direction.

6. Conclusions

The above analysis of repeated aircraft runs at 33 m over a flat surface of well-defined irrigated fields has illustrated the complexity of the spatial distribution of the measured ozone fluxes. While the spatial distributions of heat, moisture, and carbon dioxide fluxes are closely related to variations of the surface vegetation, the ozone flux exhibits small scale variations only weakly related to the NDVI.

This variability can be explained by chemical reactions of ozone. The two largest distinct maxima of the downward ozone

flux were found to be above pumping stations using diesel engines. This study shows that the spatially averaged ozone flux can significantly overestimate the deposition of the ozone flux to the natural vegetated surface in the presence of ozone loss due to NO release.

Acknowledgments. We express our appreciation to Richard Pearson Jr. for helpful discussions, Marvin Wesely and an anonymous reviewer for helpful comments on the manuscript, and Donald Stedman for insights on possible point sources. We also gratefully acknowledge Dennis Tristao for information on the two pumping systems and Jim Pederson for supplemental data. This material is based upon work supported by grant ATM-9310576 from the Physical Meteorology Program of the National Science Foundation and grant DAAH04-93-G-0019 from the Army Research Office. The field program and analysis was sponsored by California Air Resources Board. Funding for the Twin Otter research aircraft was provided by the San Joaquin Valley Air Pollution Study Agency, in collaboration with the Pacific Gas and Electric Company, the Electric Power Research Institute and the California Air Resources Board, and by the National Research Council of Canada.

References

Chamberlain, A. C., Deposition of gases and particles on vegetation and soils, in *Air Pollutants and Their Effects on the Terrestrial Ecosystem*, edited by A. H. Legge and S. V. Krupa, pp. 189–209, John Wiley, New York, 1986.

Doran, J. C., et al., The Boardman Regional Flux Experiment, *Bull. Am. Meteorol. Soc.*, *73*, 1785–1795, 1992.

Fackrell, J. E., and A. G. Robins, Concentration fluctuations and fluxes in plumes from point sources in a turbulent boundary layer, *J. Fluid Mech.*, *117*, 1–26, 1982.

Fitzjarrald, D. R., and D. H. Lenschow, Mean concentration and flux profiles for chemically reactive species in the atmospheric surface layer, *Atmos. Environ.*, *17*, 2505–2512, 1983.

Gifford, F. A., Statistical properties of a fluctuating plume dispersion model, *Adv. Geophys.*, *6*, 117–138, 1959.

Kramm, G., H. Muller, D. Fowler, K. D. Hofken, F. X. Meixner, and E. Schaller, A modified profile method for determining the vertical fluxes of NO, NO_2, ozone, and HNO_3 in the atmospheric surface layer, *J. Atmos. Chem.*, *13*, 265–288, 1991.

Lenschow, D. H., Reactive trace species in the boundary layer from a micro-meteorological perspective, *J. Meteorol. Soc. Jpn.*, *60*, 472–480, 1982.

Lenschow, D. H., Micrometeorological techniques for measuring biosphere-atmosphere trace gas exchange, in *Biogenic Trace Gases: Measuring Emissions From Soil and Water*, edited by P. A. Matson and R. C. Harriss, chap. 5, pp. 126–163, Blackwell Sci., Cambridge, Mass., 1995.

Lenschow, D. H., and A. C. Delany, An analytic formulation for NO and NO_2 flux profiles in the atmospheric surface layer, *J. Atmos. Chem.*, *5*, 301–309, 1987.

Lenschow, D. H., R. Pearson Jr., and B. B. Stankov, Estimating the ozone budget in the boundary layer by use of aircraft measurements of ozone eddy flux and mean concentration, *J. Geophys. Res.*, *86*, 7291–7297, 1981.

Leuning, R., H. H. Neumann, and G. W. Thurtell, Ozone uptake by corn (*Zea mays L.*): A general approach, *Agric. Meteorol.*, *20*, 115–135, 1979.

MacPherson, J. I., NRC Twin Otter operations in the 1991 California Ozone Deposition Experiment, *Rep. LTR-FR-118*, Flight Res. Lab., Natl. Res. Counc., Ottawa, 1992.

MacPherson, J. I., R. W. H. Schmidt, A. M. Jochum, R. Pearson Jr., H. H. Neumann, and G. den Hartog, Ozone flux measurement on the NRC Twin Otter during the 1991 California Ozone Deposition Experiment, paper presented at Eighth Symposium on Meteorological Observations, Am. Meteorol. Soc., Anaheim, Calif., 1993.

Mahrt, L., R. Desjardins, and J. I. MacPherson, Observations of fluxes over heterogeneous surfaces, *Boundary Layer Meteorol.*, *67*, 345–367, 1994.

Mann, J., and D. H. Lenschow, Errors in airborne flux measurement, *J. Geophys. Res.*, *99*, 14,519–14,526, 1994.

Massman, W. J., J. Pederson, A. Delany, G. den Hartog, D. Grantz, and R. Pearson Jr., A comparison of independent determinations of the canopy conductance for carbon dioxide, water vapor, and ozone exchange at selected sites in the San Joaquin Valley of California, paper presented at Conference on Hydroclimatology: Land-Surface/Atmosphere Interactions on Global and Regional Scales. Am. Meteorol. Soc., Anaheim, Calif., 1992.

Massman, W. J., J. Pederson, A. Delany, D. Grantz, G. den Hartog, H. H. Neumann, S. P. Oncley, R. Pearson Jr., and R. H. Shaw, An evaluation of the regional acid deposition model surface module for ozone uptake at three sites in the San Joaquin Valley of California, *J. Geophys. Res.*, *99*, 8281–8294, 1994.

McLaughlin, S. B., and G. E. Taylor, Relative humidity: Important modifier of pollutant uptake by plants, *Science*, *211*, 167–169, 1981.

Neu, U., T. Kunzle, and H. Wanner, On the relationship between ozone storage in the residual layer and daily variation in near-surface ozone concentration—A case study, *Boundary Layer Meteorol.*, *69*, 221–247, 1994.

Pearson, R., Jr., and D. H. Stedman, Instrumentation for the fast response ozone measurements from aircraft, *Atmos. Tech.*, *12*, 51–55, 1980. (Available from Natl. Cent. for Atmos. Res., Boulder, Colo.)

Schmidt, R. W. H., A. M. Jochum, and N. Enisirasser, Airborne ozone flux measurements using a new fast response detector, paper presented at *Seventh Symposium on Meteorological Observations and Instrumentation*, Am. Meteorol. Soc., New Orleans, La., 1991.

Seinfeld, J. H., *Atmospheric Chemistry and Physics of Air Pollution*, 738 pp., J. Wiley, New York, 1986.

Sun, J. and L. Mahrt, Spatial distribution of surface fluxes estimated from remotely sensed variables, *J. Appl. Meteorol.*, *33*, 1341–1353, 1994.

Taylor, G. I., Diffusion by continuous movements, *Proc. London Math. Soc.*, *Ser. 2*, *20*, 196–212, 1921.

Tucker, C. J., Red and photographic infrared linear combinations for monitoring vegetation, *Remote Sens. Environ.*, *8*, 127–150, 1979.

van Ulden, A. P., Simple estimates for vertical diffusion from sources near the ground, *Atmos. Environ.*, *12*, 2125–2129, 1978.

Venkatram, A., Dispersion in the stable boundary layer, in *Lectures on Air Pollution Modeling*, edited by A. Venkatram and J. C. Wyngaard, pp. 229–265, Am. Meteorol. Soc., Boston, Mass., 1988.

Wesely, M. R., Turbulent transport of ozone to surfaces common in the eastern half of the United States, in *Trace Atmospheric Constituents: Properties, Transformations, and Fates*, edited by S. E. Schwartz, pp. 345–370, John Wiley, New York, 1983.

Wesely, M. R., D. R. Cook, and R. W. Williams, Field measurement of small ozone fluxes to snow, wet bare soil, and lake water, *Boundary Layer Meteorol.*, *20*, 459–471, 1981.

R. L. Desjardins, Land Resources Research Centre, Agriculture Canada, Ottawa, Ontario, Canada K1A 0O6.

D. H. Lenschow, National Center for Atmospheric Research, P. O. Box 3000, Boulder, CO 80307.

J. I. MacPherson, Flight Research Laboratory, National Research Council, Ottawa, Ontario, Canada K1A 0O6.

L. Mahrt, College of Oceanic and Atmospheric Sciences, Oregon State University, Corvallis, OR 97331-2209.

J. Sun, Program in Atmospheric and Oceanic Sciences, University of Colorado, Boulder, CO 80309.

J. C. Weil, Cooperative Institute for Research in Environmental Sciences, University of Colorado, Boulder, CO 80309.

(Received January 4, 1995; revised August 4, 1995;
accepted August 23, 1995.)